APS physics

CHORUS

This is the accepted manuscript made available via CHORUS. The article has been published as:

Crossover from the Ultracold to the Quasiclassical Regime in State-Selected Photodissociation

S. S. Kondov, C.-H. Lee, M. McDonald, B. H. McGuyer, I. Majewska, R. Moszynski, and T. Zelevinsky

Phys. Rev. Lett. **121**, 143401 — Published 2 October 2018

DOI: 10.1103/PhysRevLett.121.143401

Crossover from the Ultracold to the Quasiclassical Regime in State-Selected Photodissociation

S. S. Kondov,[1] C.-H. Lee,[1] M. McDonald,[1,*] B. H. McGuyer,[1,†] I. Majewska,[2] R. Moszynski,[2] and T. Zelevinsky[1,‡]

[1] *Department of Physics, Columbia University, 538 West 120th Street, New York, NY 10027-5255, USA*

[2] *Quantum Chemistry Laboratory, Department of Chemistry, University of Warsaw, Pasteura 1, 02-093 Warsaw, Poland*

(Dated: August 9, 2018)

Processes that break molecular bonds are typically observed with molecules occupying a mixture of quantum states and successfully described with quasiclassical models, while a few studies have explored the distinctly quantum mechanical low-energy regime. Here we use photodissociation of diatomic strontium molecules to demonstrate the crossover from the ultracold, quantum regime where photofragment angular distributions strongly depend on the kinetic energy to the quasiclassical regime. Using time-of-flight imaging for photodissociation channels with millikelvin reaction barriers, we explore photofragment energies in the 0.1-300 mK range experimentally and up to 3 K theoretically, and discuss the energy scale at which the crossover occurs. We find that the effects of quantum statistics can unexpectedly persist to high photodissociation energies.

Recent progress in atomic and molecular physics has resulted in the development of an unprecedented degree of control over molecular degrees of freedom. This includes targeted preparation of molecular samples in specific internal and motional states. The ability to create molecular samples at a range of low temperatures has enabled detailed studies of few-body chemistry in the regime where quantum mechanical effects, such as resonant scattering and barrier tunneling, define the reaction cross sections.

Approaches to exploring the formation and breaking of molecular bonds across the low-energy regime include photoassociation [1], ultracold atomic collisions [2, 3], ultracold molecular collisions [4], state-selected molecular beams with relative velocity control [5–10], and molecule collisions with trapped ions [11]. Each method has its benefits such as tunability of collision energies, access to ultralow energies, or adaptability to diverse molecular species. We study molecular photodissociation [12] in the ultracold regime as a path to detailed quantitative understanding of ultracold chemistry phenomena [13]. If the molecules are trapped at sub-millikelvin temperatures, optical control of the bond breaking process allows to reach the near-threshold regime with high energy resolution and tunability. The resolution is limited only by the natural lifetime of the photofragments and the initial trap temperature (both typically < 5 mK, and in this work ~ 1 μK), and the tunability only by the laser intensity and field of view. This half-collision technique permits studies of any collisional thresholds that can be reached with one or a few photons, even those with short natural lifetimes that would prevent a successful measurement in a scattering configuration.

Previously we reported photodissociation of ultracold Sr_2 molecules in the near-threshold quantum regime [13] including interference of photofragment matter waves, sensitivity to reaction barriers, shape resonances, and control of reactions by magnetic fields [14]. Not surprisingly, the measured photofragment angular distributions disagreed with quasiclassical intuition to varying degrees [13]. It remained an open question whether a crossover into quasiclassical behavior could be observed and explained from first principles. Here, we observe the crossover from the ultracold, quantum mechanical to the quasiclassical regime of photodissociation. We show that photofragment angular distributions exhibit strong variations with the continuum energy near threshold, but stabilize to energy-independent quasiclassical patterns at energies that exceed reaction barrier heights. Our study includes an electronically excited multichannel continuum in addition to the ground-state continuum. Furthermore, we find that quantum statistics of the photofragments can prevent the photodissociation outcome from reaching the quasiclassical limit even at high energies. In the companion article [15] we show that photodissociation of very weakly bound molecules can exhibit quantum mechanical behavior to higher energies, and we explicitly compare different levels of approximation for predicting the photofragment angular distributions [16–21].

In the experiment, ^{88}Sr atoms are laser cooled and photoassociated in a one-dimensional optical lattice, yielding $\sim 7,000$ Sr_2 molecules trapped at a few microkelvin [22]. The lattice at the wavelength of 910 nm has 30 μm radius and 730 μm length. The molecules predominantly occupy the most weakly bound vibrational level, $v = -1$, in the electronic ground state that correlates to the atomic $^1S + {}^1S$ threshold. They are distributed between two angular momenta $J_i = \{0, 2\}$, either of which can be chosen as the initial state for photodissociation, with selectivity of the projection quantum number M_i. Alternatively, weakly bound levels that correlate to the excited $^1S + {}^3P_1$ continuum can be populated prior to photodissociation by 689 nm light that co-propagates with the lattice, in which case the (J_i, M_i) notation would refer to these initial bound states. The photodissociation light pulses are 10-20 μs long, the photofragment time of flight varies

from 800 μs near threshold to 20 μs at higher energies, and the imaging pulse is 10-20 μs. The absorption imaging beam is resonant with the strong 461 nm Sr transition, nearly co-aligned with the lattice, and expanded to 300 μm in order to intercept the outgoing photofragments [13]. The (vertical) quantization axis is set by the lattice polarization, or by a 3 G magnetic field when required for state selection, while the photodissociation light has polarization that is parallel ($P = 0$) or perpendicular ($P = 1$) to this axis. The continuum energy is determined by the frequency of the photodissociation light. Reaching high energies can be challenging because of diminishing bound-continuum transition strengths and rapid expansion of the photofragments.

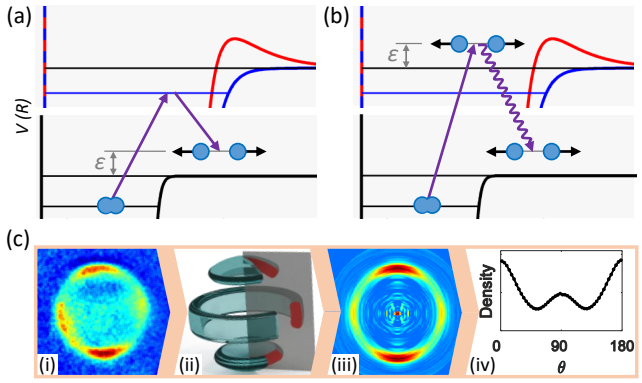

FIG. 1. (a) Schematic of Sr_2 molecule photodissociation to the ground continuum. Weakly bound molecules are fragmented with a resonant two-photon process via the excited electronic state, which effectively serves as the initial molecular state. The photofragments have total energy ε that is determined by the bound-continuum laser frequency, and are detected with absorption imaging. (b) One-photon photodissociation to the excited continuum that corresponds to a pair of interatomic potentials, 0_u^+ and 1_u, where 1_u has an electronic barrier. The excited atomic fragments radiatively decay to the ground state, and the angular distributions can be imaged as in (a). (c) Data analysis for azimuthally symmetric photofragment distributions. A time-of-flight absorption image of photofragments, typically 0.3-0.5 mm in diameter (i) where some asymmetry is introduced by inhomogeneities in the imaging beam profile, is a line-of-sight integral of the three-dimensional distribution (ii, shown as a schematic surface of constant density). A cross section of this distribution, shown in red, is retrieved from the data as in (iii) by slightly rotating the image and assuming symmetry about the horizontal axis, and radially averaged to yield an angular density profile (iv).

Figure 1(a,b) shows two photodissociation processes studied in this work. In case (a), a single molecular quantum state (v, J_i, M_i) of the $\{0_u^+, 1_u\}$ electronic manifold is resonantly populated and immediately photodissociated to the ground continuum $X0_g^+$, while process (b) samples the electronically excited continuum from a single ground quantum state. The upper continuum has contributions from the barrierless 0_u^+ potential and the 1_u potential with a ~ 1 mK electronic barrier, where the potentials are labeled by Ω_i, the atomic angular momentum projection onto the internuclear axis. Rotational barriers present for all continuum states with angular momentum $J \neq 0$ are not shown. An image of a photofragment angular distribution and the data analysis procedure are illustrated in Fig. 1(c). Panels (i-iv) show a time-of-flight image, a schematic three-dimensional distribution that results in this image via line-of-sight integration, the cross section of the distribution obtained with the inverse Abel transform of the data, and the radial average of the cross section showing the measured angular photofragment density.

We explore experimentally and theoretically the crossover from ultracold to quasiclassical chemistry. In the companion article [15], we explicitly compare the applicability of a range of approximations, including the WKB approximation and a semiclassical model that considers classical rotation of the molecule during photodissociation, to the full quantum mechanical treatment. This fully quantum treatment uses Fermi's golden rule with the bound and continuum wave functions to calculate the photodissociation cross sections. It is in agreement with data across all sampled energies and for molecules in all initial quantum states, with further improvement possible only by introducing small corrections to the *ab initio* molecular potentials [23, 24]. It is necessary to use the quantum mechanical method to model our observations near threshold. At high energy, the axial recoil limit is reached, where photodissociation is much faster than molecular rotation and the photofragments emerge along the molecular axis. The questions we address here and in Ref. [15] are (1) at what energy scale do the angular distributions approach the axial recoil limit; (2) how does this scale depend on the quantum numbers and binding energy of the molecule; and (3) how can quantum state selection prevent the axial recoil limit from agreeing with quasiclassical intuition? We find that (i) near threshold, the quantum mechanical treatment correctly captures the observed photofragment angular distributions and their dependence on the continuum energy; (ii) the axial recoil limit is reached at energies that exceed any potential barriers in the continuum; (iii) for very weakly bound molecules, quantum effects can dominate to higher energies than specified in (ii); and (iv) while the axial recoil approximation is usually equivalent to the ubiquitous quasiclassical model, this is not the case if additional selection rules are imposed by bosonic or fermionic nature of the photofragments.

Figure 2 illustrates the evolution of an angular distribution as a function of the continuum energy ε for $0_u^+(v = -4, J_i = 1, M_i = 0)$ molecules and $P = 0$. This energy dependence is characteristic of near-threshold photodissociation where there is strong sensitivity to individual partial wave components of the outgoing photofragments [13]. The molecules are photodissociated over ~ 2 orders

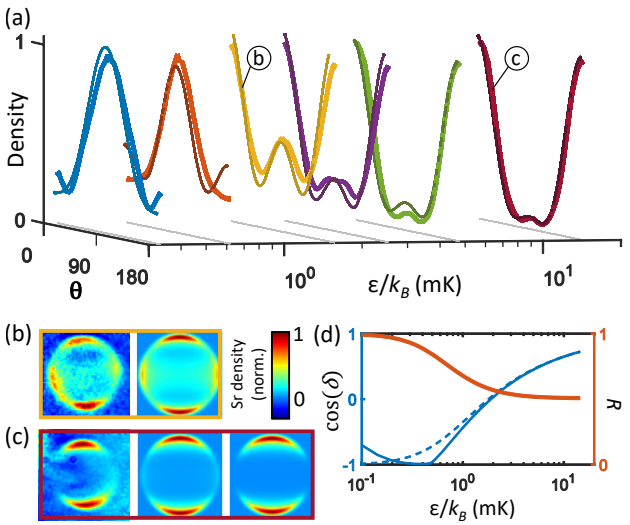

FIG. 2. (a) Angular density profiles of photofragments as a function of continuum energy, for the $0_u^+(-4,1,0)$ initial state (thick lines: experiment; thin lines: *ab initio* theory). The labeled curves correspond to panels (b,c), where curve (c) nearly matches the quasiclassical expectation. (b) Photofragment absorption image and quantum chemistry calculation for the process in (a) at the continuum energy $\varepsilon/k_B = 1.6$ mK ($\varepsilon/h = 33$ MHz; h is the Planck constant) where quantum mechanical behavior dominates. (c) Absorption image for $\varepsilon/k_B = 14$ mK ($\varepsilon/h = 300$ MHz) on the left, with the corresponding quantum chemistry model, and the axial recoil limit on the right. (d) Calculated energy evolution of R (thick line) and $\cos\delta$ (thin solid line) for the process in (a-c). The thin dashed line shows the WKB approximation and indicates its agreement with the quantum theory at $\varepsilon/k_B \gtrsim 1$ mK.

of magnitude of energy, with Fig. 2(a) displaying the angular photofragment densities as a function of ε/k_B where k_B is the Boltzmann constant. Quantum chemistry calculations of the expected density curves, based on *ab initio* Sr_2 potentials [23, 24], are overlayed with the data. The measured images for $\varepsilon/k_B = 1.6$ and 14 mK are shown in the leftmost panels of Fig. 2(b,c), followed by theoretical images. Figure 2(c) also shows an image calculated for the axial recoil limit, which is already approached at 14 mK. The angular distribution in the axial recoil limit, $I_{\rm AR}(\theta,\phi)$, agrees with the quasiclassical model: $I_{\rm AR}(\theta,\phi) = I_{\rm QC}(\theta,\phi)$. The quasiclassical model predicts the angular distribution as a product of the initial molecular orientation probability density $P_i(\theta,\phi)$ that is a function of the polar and azimuthal angles $\{\theta,\phi\}$ referenced to the quantization axis, and the angular probability density of the electric-dipole light absorption, $I_{\rm QC}(\theta,\phi) \propto P_i(\theta,\phi)[1+\beta_2 P_2(\cos\theta)]$ [17, 18]. Here P_2 is the Legendre polynomial and β_2 is the anisotropy parameter such that $\beta_2 = 2$ for a parallel photodissociation transition ($\Delta\Omega = 0$) resulting in a photofragment distribution mostly along the quantization axis and $\beta_2 = -1$ for a perpendicular transition ($|\Delta\Omega| = 1$) with a photofragment distribution mostly transverse to the axis.

For molecules composed of identical constituents such as bosonic ^{88}Sr atoms, spin statistics imposes selection rules on allowed angular momenta through the required symmetry under nuclear exchange. In the electronic ground state of $^{88}Sr_2$ only even J values are allowed, while in the 0_u^+ excited state only odd J values are possible. Since odd J are forbidden in the ground state, the quantum state of photofragments in this continuum (Fig. 1(a)) can be described by only two parameters $\{R,\delta\}$ such that the amplitudes of finding the photofragments in $J = J_i - 1$ and $J = J_i + 1$ are $\sqrt{R}$ and $\sqrt{1-R}$, respectively, with the phase difference δ. The energy evolution of R and δ is plotted in Fig. 2(d). In the axial recoil limit, $R \approx 1/2$ and $\cos\delta = 1$, as discussed in more detail in Ref. [15]. While the angular distributions in Fig. 2(a-c) and $\{R,\delta\}$ in Fig. 2(d) show a strong dependence on ε/k_B up to ~ 5 mK, at higher energies significantly exceeding the rotational barrier heights the distributions become quasiclassical, with R showing faster convergence than δ. The experiments were performed for a range of weakly bound 0_u^+ and 1_u states [15], confirming this convergence as well as the initial-state-dependent evolution for lower energies. For 1_u molecules, due to the perpendicular nature of the transition to the ground state, at high energies the fragments emerge mostly horizontally (at 90° to the light polarization) rather than vertically as for 0_u^+ in Fig. 2(b,c).

Quantum statistics of photofragments can affect the reaction outcome. For example, in photodissociation of state-selected $^{88}Sr_2$ molecules to the ground-state continuum some reaction channels (odd partial waves J) are excluded. This inherently quantum effect influences the photofragment distributions even at high energies. We investigate this phenomenon by measuring and calculating the angular distributions for the photodissociation pathway in Fig. 1(a) with $\Omega_i = 1$. We find that unless $M_i = 0$ and $P = 0$ [15], the quantum mechanical angular distributions do not match quasiclassical predictions in the high-energy limit.

Figure 3 shows two examples of photodissociation for selected initial states such that the resulting angular distributions do not converge to the quasiclassical expectation. In Fig. 3(a), the $1_u(-1,1,0)$ molecules are dissociated at 0.63 and 2.5 mK (13 and 53 MHz) above threshold. Due to the $\Delta M = \pm 1$ selection rule for $P = 1$ photodissociation of this initial state, only $J = 2$ is possible for the ground-state continuum (odd J are not allowed), and therefore no partial-wave interference or energy dependence is expected. The observations confirm an unchanging angular distribution that matches the quantum mechanical prediction and clearly fails to match the quasiclassical model. Figure 3(b) illustrates energy-dependent photodissociation of $1_u(-1,3,0)$ molecules. Here, the near-threshold energy dependence arises from

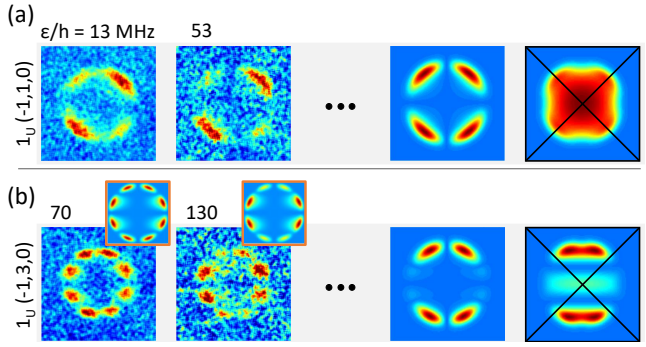

FIG. 3. Quantum statistics of identical particles prevents agreement with quasiclassical predictions at large photofragment energies. Here, $P = 1$. (a) Photofragment angular distributions for $1_u(-1,1,0)$ molecules at $\varepsilon/k_B = \{0.63, 2.5\}$ mK ($\varepsilon/h = \{13, 53\}$ MHz) on the left along with quantum mechanical and quasiclassical predictions on the right. This case is energy-independent. The quasiclassical picture fails to describe the process due to quantum statistics that leads to the missing $J = 1$ partial wave in the ground-state continuum. (b) Energy-dependent angular distributions for $1_u(-1,3,0)$ molecules at $\varepsilon/k_B = \{3.4, 6.3\}$ mK ($\varepsilon/h = \{70, 130\}$ MHz) are on the left, where the insets show the corresponding calculations. High-energy quantum mechanical and quasiclassical predictions are on the right. While the highest energy regime could not be reached experimentally, at lower energies the experiment fully agrees with quantum mechanical calculations in the insets.

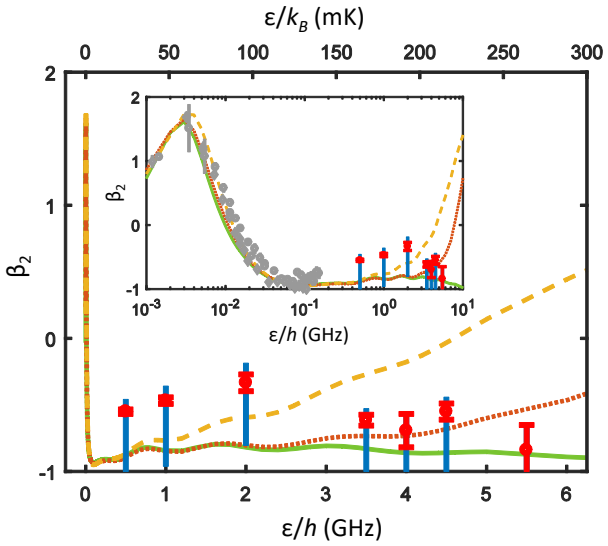

FIG. 4. Anisotropy parameter β_2 measured for photodissociation of ground-state $X0_g^+(-1,0,0)$ molecules to the excited $\{0_u^+, 1_u\}$ continuum. Red capped error bars are determined from a bootstrap analysis of up to 1,000 experimental realizations, and blue capless error bars result from possible contamination by molecules initially in $J_i = 2$. Dotted red line corresponds to the *ab initio* molecular potential [23], solid green line to the potential that is optimized to reproduce long-range properties [24], and dashed yellow line to the *ab initio* potential that was manually fitted for better agreement with measured spectra [25]. Photodissociation of these very weakly bound molecules does not yet reach the high-energy limit of $\beta_2 = 2$ at the accessible continuum energies up to 260 mK (5.5 GHz). The inset shows the high-energy data in the context of previous measurements [13] with improved *ab initio* theory.

interference of the $J = 2$ and $J = 4$ continuum states. The right-hand panels show the calculated quantum mechanical angular distribution in the axial recoil limit that disagrees with the quasiclassical model. To demonstrate experimental agreement with the quantum mechanical treatment, the left-hand side shows angular distributions at 3.4 and 6.3 mK (70 and 130 MHz) above threshold that match the calculated distributions in the insets. While the axial recoil regime (> 50 mK) was not reached in this case due to weak bound-continuum transition strengths and insufficient photodissociation laser power, this limitation is not fundamental. Note that if optical selection rules (rather than spin-statistics restrictions) allow only a single partial wave J in the continuum, then quantum mechanical and quasiclassical angular distributions strictly agree [13].

A key feature of photodissociation is the ability to select one of many possible continua. In Fig. 4 we photodissociate ground-state $X0_g^+(-1,0,0)$ molecules to the $\{0_u^+, 1_u\}$ continuum, and sample energies in the range of 0.07-260 mK (1.5-5,500 MHz). Here the electronic potential barrier height is only ~ 1 mK, being proportional to the very small C_3 dispersion coefficient that is determined by the inverse of the metastable $^3P_1$ atomic lifetime. The photofragments have angular momentum $J = 1$ and two possible $\Omega = \{0, 1\}$ that are mixed via nonadiabatic Coriolis coupling, especially at the lower energies [26]. This mixing has a strong and nontrivial effect on photofragment angular distributions. For the spherically symmetrical initial molecular state, the angular distributions can be described as $I_{\rm QC}(\theta)$ for all continuum energies, but with a varying $\beta_2(\varepsilon)$ that becomes constant at the axial recoil limit. Figure 4 shows the plot of $\beta_2(\varepsilon)$ across a wide energy range that is limited only by the photodissociation laser power, where the smaller error bars arise from the image quality and the larger ones conservatively estimate possible contamination by molecules initially in $J_i = 2$. In the case of mixed Ω in the continuum, the quasiclassical picture does not predict which Ω dominates at high energy and whether the observed pattern tends to a perpendicular (for $\Omega = 1$) or a parallel (for $\Omega = 0$) dipole. In the experiment of Fig. 4, the *ab initio* pattern tends to a parallel dipole ($\beta_2 = 2$) in the axial recoil limit, but for the very weakly bound molecules this regime is expected to be reached only at > 0.5 K above threshold. In the energy regime that is currently accessible, photofragment angular distributions vary steeply with energy in the region of the ~ 1 mK electronic barrier, then stabilize at $\beta_2 \approx -1$. The energy interval where $\beta_2 \approx -1$ is sensitive

to long-range molecular potentials, as we have confirmed by adjusting the C_6 coefficients. The measurements in this energy regime allow us to distinguish between the *ab initio* [23], long-range [24], and fitted *ab initio* [25] potentials to which the angular distributions are sensitive, as shown in Fig. 4.

In conclusion, we have explored how ultracold, quantum mechanical state-selected photodissociation crosses over into the classical regime at increasing photofragment energies. The question of applicability of quasiclassical descriptions to photodissociation reactions has lingered in the literature for several decades [13, 16, 19, 20, 27], and in this work we experimentally access and probe the range of energies where the onset of the quasiclassical regime is expected. As further detailed in Ref. [15], we find that the high-energy axial recoil limit is reached when the continuum energy exceeds any electronic and rotational barriers, although quantum effects can dominate to larger energies for very weakly bound molecules. We experimentally confirm with Sr_2 molecules that the commonly used quasiclassical formula for photofragment angular distributions [17–19] correctly describes the axial recoil limit for a variety of initial molecular states, while in the ultracold regime there is a strong nonclassical variation of the angular distributions with energy. We demonstrate that the effects of spin statistics for identical photofragments can persist to indefinitely large photodissociation energies and prevent the angular distributions from approaching the quasiclassical picture. We probe a molecular continuum with a mixture of Ω quantum numbers in an energy range of over three orders of magnitude, resolving between the *ab initio* potentials and those that have been adjusted using molecular spectroscopy. Photodissociation of ultracold molecules with isolated quantum states uniquely enables studies of molecular continua, and for relatively simple molecules such as Sr_2, state-of-the-art quantum chemistry theory yields excellent agreement with measurements. These features allow us to directly observe and accurately model the crossover from ultracold to quasiclassical chemistry.

We acknowledge the ONR Grants No. N00014-17-1-2246 and N00014-16-1-2224, as well as the NSF Grant No. PHY-1349725. R. M. and I. M. also acknowledge the Polish National Science Center Grant No. 2016/20/W/ST4/00314 and M. M. the NSF IGERT Grant No. DGE-1069240. We are grateful to C. Liedl and K. H. Leung for contributions to the experiment.

* Present address: Department of Physics, University of Chicago, 929 East 57th Street GCIS ESB11, Chicago, IL 60637, USA

† Present address: Facebook, Inc., 1 Hacker Way, Menlo Park, CA 94025, USA

‡ tanya.zelevinsky@columbia.edu

[1] K. M. Jones, E. Tiesinga, P. D. Lett, and P. S. Julienne, "Ultracold photoassociation spectroscopy: Long-range molecules and atomic scattering," Rev. Mod. Phys. **78**, 483–535 (2006).

[2] J. Wolf, M. Deiß, A. Krükow, E. Tiemann, B. P. Ruzie, Y. Wang, J. P. D'Incao, P. S. Julienne, and J. Hecker Denschlag, "State-to-state chemistry for three-body recombination in an ultracold rubidium gas," Science **358**, 921–924 (2017).

[3] R. Thomas, K. O. Roberts, E. Tiesinga, A. C. J. Wade, P. B. Blakie, A. B. Deb, and N. Kjaergaard, "Multiple scattering dynamics of fermions at an isolated p-wave resonance," Nat. Commun. **7**, 12069 (2016).

[4] S. Ospelkaus, K.-K. Ni, D. Wang, M. H. G. de Miranda, B. Neyenhuis, G. Quéméner, P. S. Julienne, J. L. Bohn, D. S. Jin, and J. Ye, "Quantum-State Controlled Chemical Reactions of Ultracold Potassium-Rubidium Molecules," Science **327**, 853 (2010).

[5] W. E. Perreault, N. Mukherjee, and R. N. Zare, "Quantum control of molecular collisions at 1 kelvin," Science **358**, 356–359 (2017).

[6] J. J. Gilijamse, S. Hoekstra, S. Y. T. van de Meerakker, G. C. Groenenboom, and G. Meijer, "Near-threshold inelastic collisions using molecular beams with a tunable velocity," Science **313**, 1617–1620 (2006).

[7] S. N. Vogels, J. Onvlee, S. Chefdeville, A. van der Avoird, G. C. Groenenboom, and S. Y. T. van de Meerakker, "Imaging resonances in low-energy NO-He inelastic collisions," Science **350**, 787–790 (2015).

[8] A. Klein, Y. Shagam, W. Skomorowski, P. S. Żuchowski, M. Pawlak, L. M. C. Janssen, N. Moiseyev, S. Y. T. van de Meerakker, A. van der Avoird, C. P. Koch, and E. Narevicius, "Directly probing anisotropy in atom-molecule collisions through quantum scattering resonances," Nature Phys. **13**, 35–38 (2017).

[9] A. P. P. van der Poel, P. C. Zieger, S. Y. T. van de Meerakker, J. Loreau, A. van der Avoird, and H. L. Bethlem, "Cold collisions in a molecular synchrotron," Phys. Rev. Lett. **120**, 033402 (2018).

[10] X. Wu, T. Gantner, M. Koller, M. Zeppenfeld, S. Chervenkov, and G. Rempe, "A cryofuge for cold-collision experiments with slow polar molecules," Science **358**, 645–648 (2017).

[11] S. Willitsch, M. T. Bell, A. D. Gingell, S. R. Procter, and T. P. Softley, "Cold reactive collisions between laser-cooled ions and velocity-selected neutral molecules," Phys. Rev. Lett. **100**, 043203 (2008).

[12] H. Sato, "Photodissociation of simple molecules in the gas phase," Chem. Rev. **101**, 2687–2725 (2001).

[13] M. McDonald, B. H. McGuyer, F. Apfelbeck, C.-H. Lee, I. Majewska, R. Moszynski, and T. Zelevinsky, "Photodissociation of ultracold diatomic strontium molecules with quantum state control," Nature **534**, 122–126 (2016).

[14] M. McDonald, I. Majewska, C.-H. Lee, S. S. Kondov, B. H. McGuyer, R. Moszynski, and T. Zelevinsky, "Control of ultracold photodissociation with magnetic fields," Phys. Rev. Lett. **120**, 033201 (2018).

[15] I. Majewska, S. S. Kondov, C.-H. Lee, M. McDonald, B. H. McGuyer, R. Moszynski, and T. Zelevinsky, "Experimental and theoretical investigation of the crossover from the ultracold to the quasiclassical regime of photodissociation," arXiv:1805.09482 (2018).

[16] R. N. Zare, "Photoejection dynamics," Mol. Photochem. **4**, 1–37 (1972).

[17] S. E. Choi and R. B. Bernstein, "Theory of oriented symmetric-top molecule beams: Precession, degree of orientation, and photofragmentation of rotationally state-selected molecules," J. Chem. Phys. **85**, 150–161 (1986).

[18] R. N. Zare, "Photofragment angular distributions from oriented symmetric-top precursor molecules," Chem. Phys. Lett. **156**, 1–6 (1989).

[19] T. Seideman, "The analysis of magnetic-state-selected angular distributions: a quantum mechanical form and an asymptotic approximation," Chem. Phys. Lett. **253**, 279–285 (1996).

[20] J. A. Beswick and R. N. Zare, "On the quantum and quasiclassical angular distributions of photofragments," J. Chem. Phys. **129**, 164315 (2008).

[21] E. Wrede, E. R. Wouters, M. Beckert, R. N. Dixon, and M. N. R. Ashfold, "Quasiclassical and quantum mechanical modeling of the breakdown of the axial recoil approximation observed in the near threshold photolysis of IBr and Br_2," J. Chem. Phys. **116**, 6064 (2002).

[22] G. Reinaudi, C. B. Osborn, M. McDonald, S. Kotochigova, and T. Zelevinsky, "Optical production of stable ultracold $^{88}Sr_2$ molecules," Phys. Rev. Lett. **109**, 115303 (2012).

[23] W. Skomorowski, F. Pawłowski, C. P. Koch, and R. Moszynski, "Rovibrational dynamics of the strontium molecule in the $A^1\Sigma_u^+$, $c^3\Pi_u$, and $a^3\Sigma_u^+$ manifold from state-of-the-art *ab initio* calculations," J. Chem. Phys. **136**, 194306 (2012).

[24] M. Borkowski, P. Morzyński, R. Ciuryło, P. S. Julienne, M. Yan, B. J. DeSalvo, and T. C. Killian, "Mass scaling and nonadiabatic effects in photoassociation spectroscopy of ultracold strontium atoms," Phys. Rev. A **90**, 032713 (2014).

[25] B. H. McGuyer, M. McDonald, G. Z. Iwata, M. G. Tarallo, A. T. Grier, F. Apfelbeck, and T. Zelevinsky, "High-precision spectroscopy of ultracold molecules in an optical lattice," New J. Phys. **17**, 055004 (2015).

[26] B. H. McGuyer, C. B. Osborn, M. McDonald, G. Reinaudi, W. Skomorowski, R. Moszynski, and T. Zelevinsky, "Nonadiabatic effects in ultracold molecules via anomalous linear and quadratic Zeeman shifts," Phys. Rev. Lett. **111**, 243003 (2013).

[27] R. N. Zare and D. R. Herschbach, "Doppler line shape of atomic fluorescence excited by molecular photodissociation," Proc. IEEE **51**, 173–182 (1963).